Compact Six-sector Antenna Using Three Intersecting Dual-beam Microstrip Yagi-Uda Arrays with Common Director

Naoki Honma†, Tomohiro Seki, Kenjiro Nishikawa, and Shuji Kubota

Abstract

This paper presents a novel compact planar six-sector antenna suitable for wireless terminals. Our new design yields low-profile and extremely compact multisector antennas because it allows microstrip Yagi-Uda array antennas to share director elements. Two microstrip Yagi-Uda array antennas are combined to form a unit linear array that has a feed element at each end: only one of them is excited at any one time and the other is terminated. A numerical analysis shows that applying a resistive load to the feed port of the terminated element is effective in improving the front-to-back ratio. We investigated the radiation pattern of a six-sector antenna, which uses three intersecting unit linear arrays, and identified the optimum termination condition. From the results of measurements at 5 GHz, we verified the basic properties of our antenna. It achieved high gain of at least 10 dBi, even though undesired radiation was suppressed. A radiation pattern suitable for a six-sector antenna could be obtained even with a substrate having a diameter of 1.83 wavelengths, i.e., an area 75% smaller than that of an ordinary antenna with six individual single-beam microstrip Yagi-Uda arrays in a radial configuration. We also fabricated an antenna for the 25-GHz band and found that it has potential for high antenna performance, such as antenna gain of over 10 dBi even in the quasi-millimeter band.

1. Introduction

Studies on high-speed indoor wireless access systems, which use the microwave or millimeter bands are being actively pursued [1], [2]. These systems must reduce the effect of multipath fading in order to maintain high data transmission speeds. Narrow-beam antennas and adaptive arrays can overcome this problem, and the effects of these antennas in wireless communication systems have been studied [3]–[6]. A narrow-beam antenna is the easiest way to improve the data transmission speed because a fixed-beam antenna can be used and it achieves a relatively high gain. A multisector antenna comprising several narrow-beam antennas with different beam directions is one way to provide wireless connections with a high data transmission speed because the terminals or access points can switch the beam direction so as to direct the beam to the desired signal [7]–[11].

Mobile terminals usually utilize only one sector of a multisector antenna at any one moment because only one connection to one access point is necessary. This requires the use of a sector switching mechanism. A sector antenna with too few sectors provides only a relatively low gain enhancement effect, which may be canceled by the loss that occurs in the sector switching mechanism in the feed circuit. On the other hand, a sector antenna with many sectors requires a complicated multiport sector switching mechanism. Therefore, terminals are likely to use four to six sectors [7], [10], [11]. Moreover, multisector antennas for mobile terminals must be small and low-profile because of the recent downsizing of mobile terminals for enhanced portability.

† NTT Network Innovation Laboratories
Yokosuka-shi, 239-0847 Japan
Email: honma.naoki@lab.ntt.co.jp

A low profile multisector antenna can be fabricated using radially arranged microstrip Yagi-Uda arrays [12]. A microstrip Yagi-Uda array comprises an exciting microstrip antenna and several parasitic microstrip antennas arranged on the same substrate surface. It offers high gain [13]. Furthermore, this antenna can be fabricated using etching techniques, which enables mass production. However, it usually requires a large substrate area because each sector requires an individual array antenna. The other problem with the microstrip Yagi-Uda array is the difficulty in obtaining a sufficient front-to-back ratio (F/B). The high level of undesired radiation degrades the data transmission speed [5].

In this paper, we describe a new compact planar six-sector antenna based on a microstrip Yagi-Uda array with common director elements that is suitable for mobile terminals. One of the key ideas for reducing the antenna size is a dual-beam microstrip Yagi-Uda array—a new invention for the terminal sector antenna. In this antenna, the parasitic elements are shared between two opposite-facing microstrip Yagi-Uda arrays, enabling the size of the array antenna to be reduced to almost half that of two individual microstrip Yagi-Uda arrays. Another key idea is further element sharing among the multiple linear Yagi-Uda arrays because three dual-beam Yagi-Uda arrays are necessary to obtain six beams. That is, the parasitic elements are to be shared not only by two beams, but also by all six beams. This is made possible by placing a hexagonal parasitic element at the center of the linear array, where the three unit linear arrays intersect. The optimized termination condition at the feed ports of the quiescent exciting elements is used to improve the effect of the coupling among the intersecting linear arrays. These techniques of element sharing and feed port termination yield an extremely compact six-sector antenna.

Section 2 briefly describes the basic idea of the dual-beam microstrip Yagi-Uda array antenna, in which the two exciting elements share parasitic elements. Section 3 describes the geometry and mechanism of the six-sector antenna, in which the parasitic elements are shared among six beams. Section 4 shows a numerical analysis of the six-sector antenna. We investigated the impact of the intersecting linear arrays on the radiation pattern of a six-sector antenna under various termination conditions. Section 5 describes experiments conducted on a fabricated six-sector antenna operating at 5 GHz to confirm the validity of the design. Section 6 describes the results of a trial in which this antenna was applied to the 25-GHz band. The 25-GHz band is being considered for advanced wireless local area networks (WLANs) because more frequency channels will be needed in order to offer high-speed data transmission to many more users [14].

2. Dual-beam microstrip Yagi-Uda Array with common parasitic elements

2.1 Basic geometry and mechanism

First of all, we present the idea and basic properties of the dual-beam Yagi-Uda array, which is the unit component of the six-sector antenna. We mainly examined the influence of the termination condition of the quiescent element and the number of parasitic elements.

The geometries of a conventional microstrip Yagi-Uda array and a dual-beam microstrip Yagi-Uda array, are shown in **Figs. 1(a)** and **(b)**, respectively. The microstrip antenna elements are formed on a dielectric substrate, which has ground metallization on the rear side. These elements are rectangular patches. Each array antenna has m parasitic elements aligned on the x-axis. The exciting element with the feed port at the end of the array is slightly larger than the parasitic elements.

In the figure, a and a' are the lengths of the long and

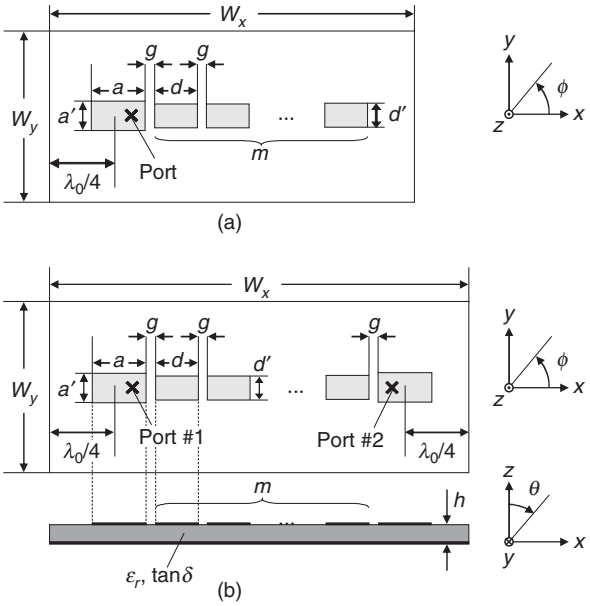

Fig. 1. Unit linear array configurations: (a) Top view of conventional microstrip Yagi-Uda array and (b) top and side views of dual-beam microstrip Yagi-Uda array.

short sides of the exciting element, respectively, d and d' are the lengths of the long and short sides of each parasitic element, respectively, g is the gap between elements, h is the thickness of the substrate, W_x and W_y are the lengths of the long and short sides of the substrate, and ε_r and $\tan\delta$ are defined as the relative dielectric constant and the loss tangent of the substrate, respectively.

The dimensions and material properties are set to $a = 0.34\ \lambda_0$, $a'/a = 0.6$, $d'/d = 0.5$, $d/a = 0.92$, $g = 0.005\ \lambda_0$, $h = 0.027\lambda_0$, $\varepsilon_r = 2.2$, and $\tan\delta = 0.0008$, where λ_0 is the wavelength in vacuum. The length of the short side of the rectangular substrate is set to $W_y = \lambda_0/2$, and W_x, which is the length of the long side, is set so that the distance between the edge of the substrate and the center of the end element in the linear array is $\lambda_0/4$.

The dual-beam microstrip Yagi-Uda array has two exciting elements, one at each end of the linear array. Each exciting element has a feed port, but only one port is driven at any one time. That is, when one port is excited, the other port is terminated.

In these antennas, the beam extends away from the exciting element over the parasitic elements, which work as a director. Therefore, the antenna shown in Fig. 1(a) can work as a single-beam Yagi-Uda array, and the antenna shown in Fig. 1(b) can work as a dual-beam Yagi-Uda array if the feed ports are switched.

2.2 Numerical analysis

The impact on antenna performance of the port termination condition and the number of parasitic elements was numerically analyzed by the method of moments (MoM). In this numerical analysis, only the dielectric layer of the substrate was assumed to be an infinite plane to simplify the analysis. The positions of the feed ports were optimized to minimize the reflection of the incident power in both models. The impedance of the terminated port #2, Z_L (load impedance), was set to the characteristic impedance of the feed line Z_0; i.e., $Z_L = Z_0 = 50\ \Omega$.

To evaluate the radiation performance as a planar sector antenna, we defined F/B and the conical radiation pattern. In this paper, F/B is defined as the ratio of the directivity of the direction of maximum radiation to that of the direction of the maximum lobe in the range of ±60° from the opposite direction. However, since the directions of both the mainlobe and the backlobe are tilted above the ground plane [12]–[13], F/B obtained in the usual way is underestimated. For this reason, we created a new definition of F/B, suitable for the configuration in Fig. 1. Our definition of F/B is shown in **Fig. 2**. The two cones are symmetrical and share the same apex. The mainlobe lies inside one cone. F/B is defined as the ratio of the maximum level in one cone to that in the direction within the other cone.

The definition of the conical plane radiation pattern is shown in **Fig. 3**. We assume a conical plane including the direction of the peak radiation. The conical-plane radiation pattern can be defined by the pattern obtained by cutting the three-dimensional pattern with an ideal conical plane. By using the conical-plane radiation pattern, we can define the conical-plane beamwidth as the range of the angle that limits the gain decrease from the maximum gain to within 3 dB.

The radiation patterns were calculated while vary-

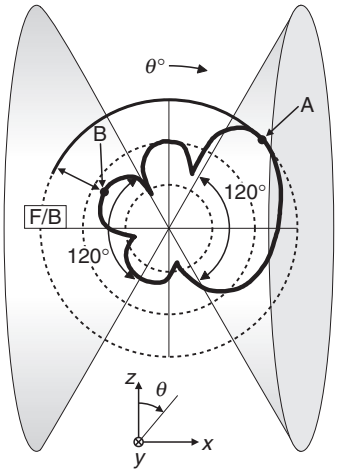

Fig. 2. Definition of F/B in this paper.

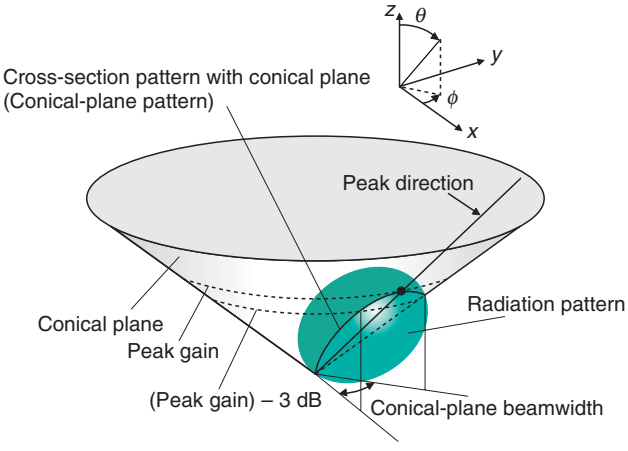

Fig. 3. Definition of conical-plane beamwidth.

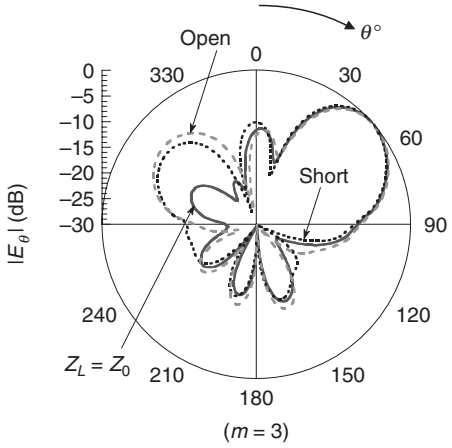

Fig. 4. Radiation pattern of unit array in *xz*-plane.

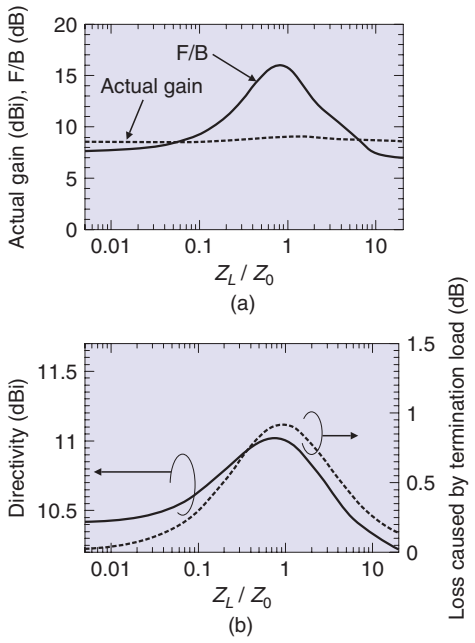

Fig. 5. Radiation properties versus load resistance: (a) Actual gain and F/B and (b) directivity and loss caused by termination load.

ing the termination condition so as to find their effect on F/B improvement. **Figure 4** shows the radiation pattern of a linear array with three parasitic elements in the *xz*-plane for three termination conditions of port #2: short, open, and $Z_L = Z_0$. The backlobe has a high level when Z_L is short or open and is reduced only when $Z_L = Z_0$. This is because the reflection of the traveling wave at the terminated port is suppressed by the termination load. To find the optimum termination condition, we calculated the relationship between the radiation pattern and impedance Z_L. **Figure 5** shows the actual gain, F/B, directivity, and termination loss versus the termination load impedance Z_L, where the number of parasitic elements is three. F/B is maximum when Z_L is around Z_0. The improvement in F/B compared with the cases of short and open termination is more than 8 dB. We also found that the directivity and termination loss are maximum when Z_L is around Z_0. By considering the slight gain difference over the range of the termination load condition shown in this graph, we can explain this as follows. The load impedance Z_L, which is almost the same as the impedance of the feed line Z_0, does not attenuate the mainlobe radiation, but does attenuate the undesired radiation caused by the reverse traveling wave, which comes up at the end of the line array. From the above calculations, we found that applying a termination load to the quiescent feed port is effective in enhancing F/B without incurring any reduction in gain.

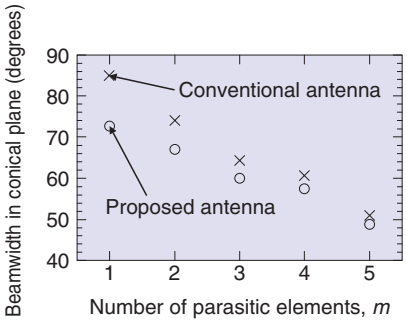

Fig. 6. Beamwidth in conical plane versus number of director elements.

To design the sector antennas, we clarified the beamwidth of the unit linear array. Numerical results for conical-plane beamwidth versus the number of parasitic elements are shown in **Fig. 6**, for the case in which port #2 is terminated by a resistor corresponding to $Z_L = Z_0 = 50\ \Omega$. We found that the beamwidth of the linear array was narrower than that of the conventional array. This means that the element terminated by Z_L also works as a director element. We also found that the linear array with three parasitic elements has a beamwidth of almost 60°, making it suitable for a six-sector antenna.

3. Geometry and mechanism of six-sector microstrip Yagi-Uda antenna with common parasitic elements

The configuration of the six-sector microstrip Yagi-Uda antenna on a circular substrate is shown in **Fig.**

7. The substrate has ground metallization on the rear side. Three unit linear arrays intersect at the center at an angle of 60°. Therefore, the shape of the central parasitic element, which is shared by all three linear arrays, is hexagonal. All of the parasitic elements are electrically smaller than the exciting elements.

In the figure, c is the width of the central hexagonal parasitic element and $c/a = 0.96$. The diameter of the substrate is $1.83\lambda_0$ when the distance between the edge of the substrate and the center of the exciting elements is set to $\lambda_0/4$. The other dimensions and material parameters shown in Fig. 7 are the same as those described in Section 2. The substrate area is only 25% of that of a conventional antenna with six individual single-beam microstrip Yagi-Uda arrays in a radial configuration. It is also much smaller than the antennas that use the techniques described in refs. [9] and [10].

The key idea of this antenna is the radiation pattern forming provided by controlling the port termination condition at all quiescent elements. For example, consider what happens when element #1 is excited and all other elements are terminated and thus quiescent. Element #1 is strongly coupled to its adjacent parasitic element, the central common parasitic element, and finally to element #4. Therefore, this linear array also works as a microstrip Yagi-Uda antenna, whose beam direction is from #1 to #4. However, this linear array is strongly coupled to the two other intersecting linear arrays, which causes undesired radiation. This undesired radiation can be suppressed by changing the termination of the quiescent elements, such as #2, #3, #5, and #6. This is discussed below.

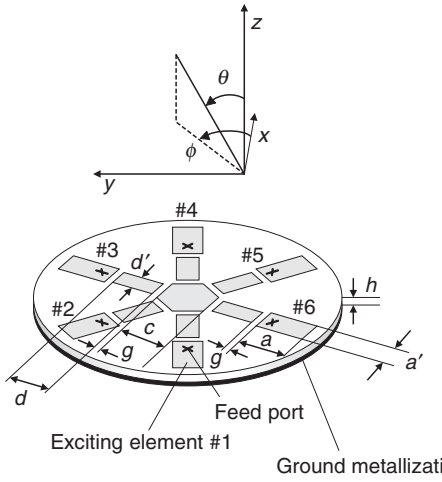

Fig. 7. Geometry of planar six-sector antenna.

4. Numerical analysis of six-sector antenna

4.1 Effect of coupling between intersecting linear arrays

In the six-sector antenna shown in Fig. 7, there is strong coupling among the three linear arrays, which impacts the radiation pattern, because all the arrays share the central parasitic element. The calculated conical radiation pattern of the antenna in Fig. 7 is shown in **Fig. 8**. In this calculation, we treated the case where all of the terminated ports are connected to loads with a value of $Z_L = Z_0$. Here, an infinite ground plane and substrate are assumed to simplify the calculation. It can be seen that the beamwidth is much larger than that of the single linear array. The actual gain and F/B of the six-sector antenna are lower than those of the single linear array by 1 and 4 dB, respectively. This means that the two other linear arrays resonate and generate undesired radiation, which degrades the radiation pattern. The scattering parameters of the six ports are listed in **Table 1**. The amounts of power transmitted from #1 to #4 and from #1 to #2 or #6 are almost the same, which indicates that the power fed to port #1 is distributed not only to the excited linear array, but also to the intersecting linear arrays at high levels. Moreover, we found that the total power consumed by the termination loads is at least 20% of the fed power. Therefore, the gain and

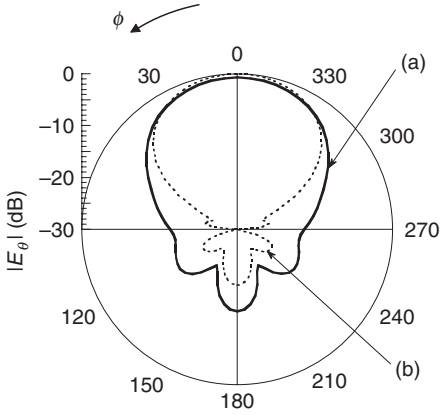

Fig. 8. Radiation patterns in conical plane ($\theta = 45°$): (a) Pattern of six-sector antenna with 50 Ω termination at all ports and (b) pattern of single linear array in Fig. 1(b) ($m = 3$).

Table 1. Calculated S-parameters in crossed array antenna.

	S_{21}	S_{31}	S_{41}	S_{51}	S_{61}
Amplitude (dB)	–10.97	–15.75	–10.80	–15.75	–10.97
Phase (deg.)	–95.5	76.0	44.0	76.0	–95.5

F/B are strongly affected by the presence of the intersecting linear arrays.

4.2 Radiation pattern improvement using reactive termination load

To improve the radiation pattern, we examined other termination conditions because the power consumed at the feed ports can be utilized by changing the termination conditions. Termination with a pure reactive load fully reflects the incident power at the feed ports without any power consumption, and the reflection phase can be controlled by changing the reactance of the load. Arbitrary reactance values can easily be obtained by attaching line stubs of various lengths. A model of the six-sector antenna with lines of length l is shown in **Fig. 9**. Each line has a single-pole three throw (SP3T) switch at its end and the switch connects the end of the line to either a signal source, resistive termination, or open termination. When one port is excited, the port at the opposite end of the array is connected to the termination load to reduce the backlobe, and all other ports are set to open. To obtain a symmetric conical radiation pattern with controllable termination conditions, all lines should be the same length. When the end of the line is open, the line works as an open stub, and its impedance Z_{in} observed at the port is expressed by

$$Z_{in} = \frac{Z_0}{j \tan \beta l}, \qquad (1)$$

where Z_0 is the characteristic impedance of the line, which is equal to the impedance of the signal source, and β is the phase constant in the line.

The calculated actual gain and beamwidth are shown as functions of line length l in **Fig. 10**. For simplification, the substrate and ground metallization were assumed to be infinite planes. The actual gain and beamwidth exhibit periodicity because the reactance of the open line at the port also changes periodically, as can be seen from Eq. (1). Note that F/B and the gain are maximum around $\beta l = n\pi$ (n = 0, 1, 2, ...) and the beamwidth is almost 60°, which is suitable for a six-sector antenna. We found that making the line length an integral multiple of the half wavelength gave the optimum radiation pattern in this six-sector antenna geometry.

5. Measurement at 5 GHz

Based on the design described above, we fabricated a six-sector antenna with $1.83\lambda_0$ and measured its characteristics. **Figure 11** shows the measured $|S_{11}|$, where ports #2, #3, #5, and #6 were open, port #4 was connected to a load of $Z_L = Z_0 = 50\ \Omega$, and $l = 0$. Here, f_c is the center frequency (5 GHz). The measured values generally agree with the calculated ones. The $|S_{11}|$ was less than –15 dB in the 6.5% bandwidth region. Resonance occurred at about f/f_c =1.11 due to the res-

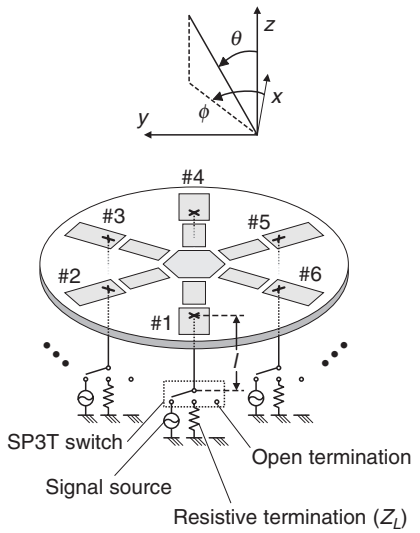

Fig. 9. Circuit configuration with finite lines and SP3T switches.

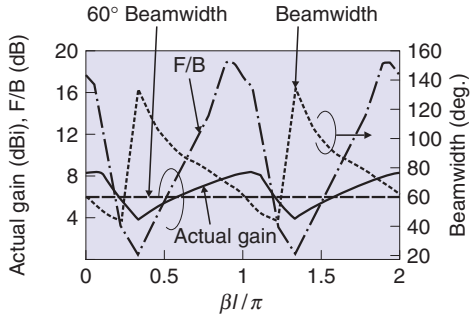

Fig. 10. Actual gain, F/B, and conical-plane beamwidth versus line length l.

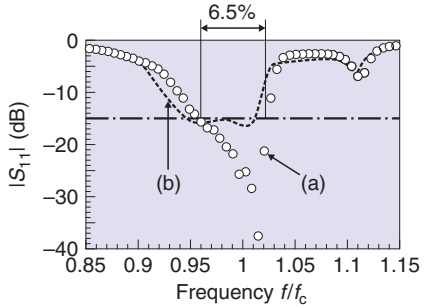

Fig. 11. $|S_{11}|$ versus frequency in six-sector antenna: (a) Measurement and (b) calculation.

onance of the rectangular parasitic elements. The loss caused by termination is shown in **Fig. 12**. The measured values also agree with the calculated ones. The termination loss was less than 1 dB and this corresponds to the result shown in Fig. 5.

Figures 13 and **14** show, respectively, the vertical radiation pattern in the *xz*-plane and the conical radiation pattern at $\theta = 45°$, which is equal to the main-lobe direction. $|E_\theta|$ and $|E_\phi|$ are defined as the co-polarization and cross-polarization components, respectively. The radiation pattern of the single linear array was also calculated to investigate the effect of the intersecting arrays on the radiation performance. For all the calculations with these models, we assumed an identical finite ground plane. $|E_\phi|$ components are not shown in Figs. 13(b) and (c) because no $|E_\phi|$ components appeared in the calculation.

The good agreement between the measured and calculated results confirms the validity of the numerical design. Moreover, the maximum cross-polarization level was 10 dB lower than the co-polarization level. The microstrip antenna's cross-polarization component in the conical plane is not low if the substrate is placed parallel to the *xy*-plane. In only the *xz*-plane, a very low level of $|E_\phi|$ component was observed when the current direction on the microstrip antenna was parallel to *x*-axis. Since the microstrip Yagi-Uda array narrows the beam toward the *xz*-plane in this case, our antenna achieved a radiation pattern with a relatively low cross-polarization level. Furthermore, comparing the radiation pattern of our antenna with

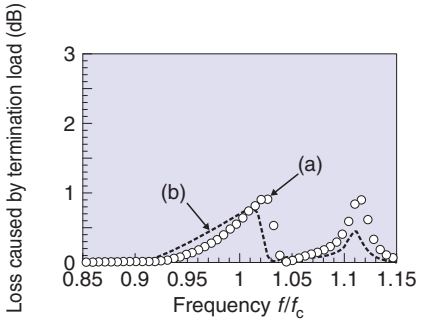

Fig. 12. Loss caused by termination versus frequency in six-sector antenna: (a) Measurement and (b) calculation.

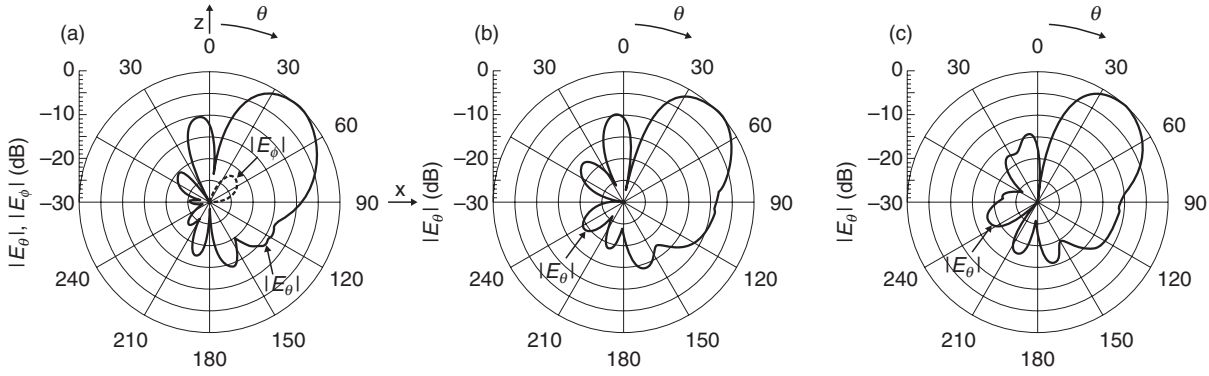

Fig. 13. Radiation patterns in vertical plane ($\phi = 0$): (a) Measurement of six-sector antenna, (b) calculation of six-sector antenna, and (c) calculation of single linear array.

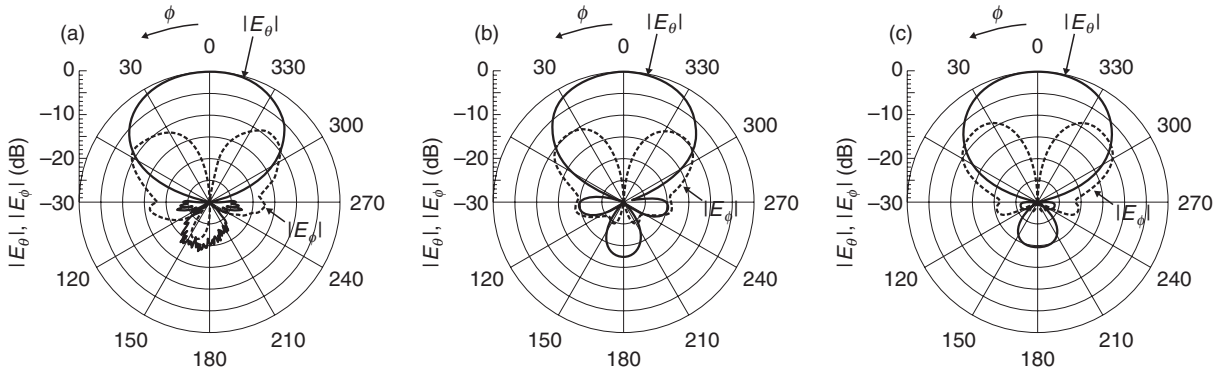

Fig. 14. Radiation patterns in conical plane ($\theta = 45°$): (a) Measurement of six-sector antenna, (b) calculation of six-sector antenna, and (c) calculation of single linear array.

that of a single linear array, we did not observed any increase in the cross-polarization component caused by the intersecting linear arrays. The reason our antenna had low cross-polarization even with the intersecting linear arrays is that its geometry is symmetrical, which helps to cancel the radiation of the cross-polarization components from the intersecting arrays. We found that we could obtain a conical-plane beamwidth of 73° and F/B of 17 dB and that this six-sector antenna has a radiation pattern suitable for a sector antenna.

The frequency dependence of the measured and calculated F/B and actual gain are shown in **Fig. 15**. For both F/B and actual gain values, the measured and calculated values agree well. F/B exceeded 17 dB and the gain exceeded 10 dBi around the center frequency. The actual gain of the six-sector antenna was 1 dB higher than that of the single linear array shown in Fig. 5. This is because of the difference in the shape of the ground plane. In our analysis, we could only treat infinitely planar substrates; such a substrate causes surface wave loss, which cannot occur in measurements. We think that the reason for the good agreement between the calculated and measured gain values is that the directivity enhancement provided by the narrow beam and the radiation efficiency degradation happen to cancel each other out in the calculation. Meanwhile, dramatic F/B deterioration was seen when $f/f_c > 1.01$ and the frequency range for 1-dB gain attenuation was $0.955 < f/f_c < 1.017$. That is, the actual available bandwidth of this antenna is about 5.5%, i.e., $0.955 < f/f_c < 1.01$.

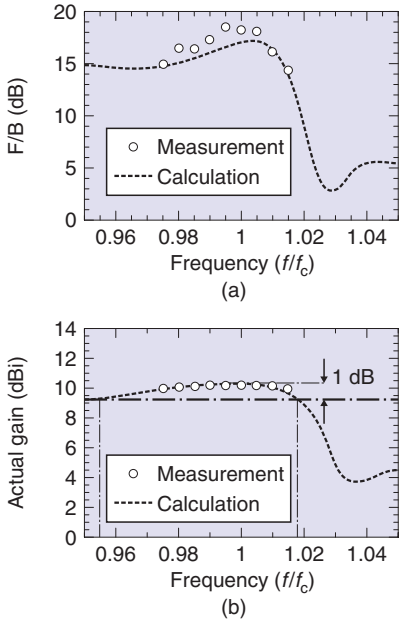

Fig. 15. Frequency dependence of antenna characteristics: (a) F/B and (b) actual gain.

6. Antenna construction and measurement at 25 GHz

We investigated a WLAN system operating at 25 GHz [14] and found that using the sector antenna is effective in maintaining the coverage area even when the propagation loss is larger than that at 5 GHz. The sector antenna design described in this paper provides a sector antenna that can be easily configured to fit within the width of a PC card. At a very high frequency, such as in the quasi-millimeter band, however, the manufacturing error will be serious because the wavelength is short and the antenna properties are changed by even small differences in antenna element size. In this section, we present the measured performance of the antenna at 25 GHz and discuss the feasibility of this antenna.

A photograph of the fabricated six-sector antenna for 25 GHz is shown in **Fig. 16**. The antenna diameter D is 22 mm and the substrate thickness h is 0.43 mm. As can be seen, the antenna's small size makes it suitable for a PC card terminal, for which the manufacturing error of the printed metal pattern on the substrate was less than 20 μm.

The measured scattering parameters of the fabricated antenna are shown in **Fig. 17**. Here, only port #1 was excited. The transmitted power was observed at port #4, and the other ports were open. The calculated values, which were obtained using MoM, show that $|S_{11}|$ is less than –10 dB over the 13% frequency range. The measured and calculated values of $|S_{41}|$ mostly agree with each other. The power wasted at the terminated port was 15% of the fed power.

Figure 18 shows the measured radiation patterns, where the conical pattern was obtained at the angle of $\theta = 45°$, which corresponds to the peak direction of

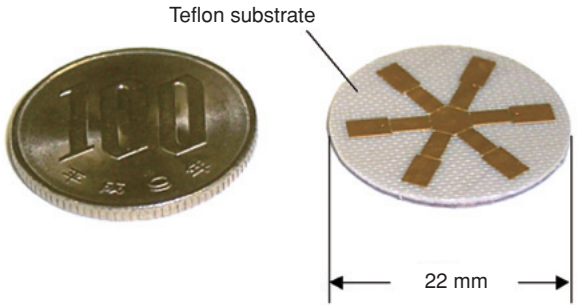

Fig. 16. Photograph of the fabricated antenna for 25 GHz.

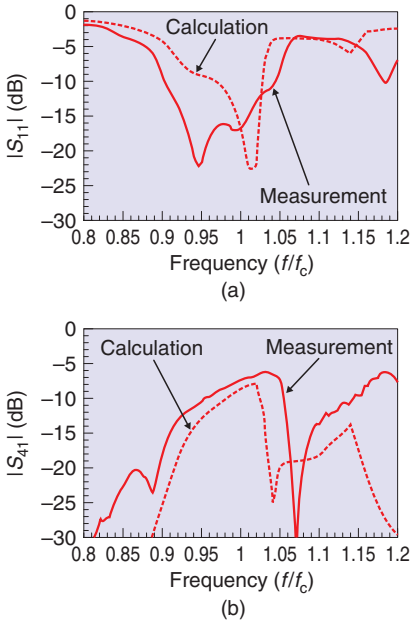

Fig. 17. Measured and calculated *S*-parameter: (a) $|S_{11}|$ and (b) $|S_{41}|$.

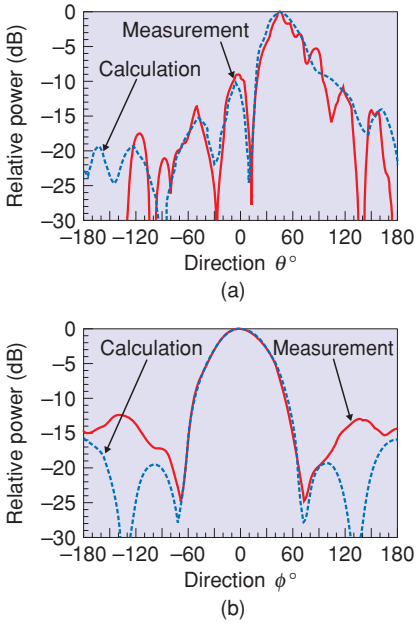

Fig. 18. Measured and calculated radiation pattern: (a) Vertical plane (*xz*-plane) and (b) conical plane ($\theta = 45°$).

the vertical plane radiation pattern. The measured and calculated radiation patterns agree well in the vertical plane, and the mainlobe shape was predicted well by calculation in the conical plane. There is a ripple in the measured vertical radiation pattern, and we suspect that this is the effect of scattering by the feeding cable. The measured peak gain of the antenna was 11.2 dBi, which is slightly higher than the result for 5 GHz. These results indicate that manufacturing error is not a serious problem and support the feasibility of our antenna.

7. Conclusion

We are studying a novel compact planar six-sector antenna that uses an array of dual-beam microstrip Yagi-Uda antennas with common directors for use in mobile terminals. A numerical analysis of the unit dual-beam array showed that terminating the quiescent ports with an appropriate load enhances the F/B value by at least 8 dB. We investigated the radiation pattern of a six-sector antenna configured by combining 3 dual-beam unit arrays. To reduce the effect of undesired coupling between unit arrays, we connected the quiescent ports of the other two unit arrays to finite-length lines that fully reflect the incident power. We found the optimum termination condition at the quiescent ports that maximizes F/B and actual gain. Based on our numerical design, we fabricated a six-sector antenna. Measured results show that it offers a high F/B value of 17 dB, high actual gain of at least 10 dBi, and a radiation pattern that is suitable for a six-sector antenna. These results indicate that our six-sector antenna offers both high radiation performance and a 75% reduction in substrate area compared with the equivalent conventional antenna with six individual microstrip Yagi-Uda arrays in a radial configuration. We also fabricated a six-sector antenna for 25 GHz. Its diameter was 22 mm and the substrate thickness was 0.43 mm. This antenna achieved a conical-plane beamwidth of 61° and actual gain of 11.2 dBi. These results indicate the feasibility of our antenna for 25-GHz operation.

Acknowledgment

We thank Professor Dr. Kunio Sawaya and Associate Professor Dr. Qiang Chen of Tohoku University and Professor Dr. Koichi Tsunekawa of Chubu University for their encouragement and advice.

References

[1] Y. Takimoto, “Recent activities on millimeter wave indoor LAN sys-

tem development in Japan," Digest of IEEE MTT-S Int. Symp., Vol. WEID-3, pp. 405–408, June 1995.
[2] N. Morinaga and A. Hashimoto, "Technical trend of multimedia mobile and broadband wireless access systems," IEICE Trans., Vol. E82-B, No. 12, pp. 1897–1905, Dec. 1999.
[3] R. W. Chang, "Synthesis of band-limited orthogonal signals for multichannel data transmission," Bell Syst. Tech. J., Vol. 45, No. 12, pp. 1775–1796, 1966.
[4] R. W. Chang and R. A. Gibby, "A Theoretical Study of Performance of an Orthogonal Multiplexing Data Transmission Scheme," IEEE Trans. Commun., Vol. COM-16, No. 4, pp. 529–540, Aug. 1968.
[5] K. Uehara, T. Seki, and K. Kagoshima, "New indoor high-speed radio communication system," IEEE Vehicular Technology Conference, Vol. 2, pp. 996–1000, July 1995.
[6] Y. Takatori, K. Cho, K. Nishimori, and T. Hori, "Adaptive Array Employing Eigenvector Beam of Maximum Eigenvalue and Fractionally-spaced TDL with Real Tap," IEICE Trans. Commun., Vol. E83-B, No. 8, pp. 1678–1687, Aug. 2000.
[7] J. E. Mitzlaff, "Radio Propagation and Anti-multipath Techniques in the WIN Environment," IEEE Network Magazine, Vol. 5, No. 6, pp. 21–26, Nov. 1991.
[8] T. Seki and T. Hori, "Cylindrical Multi-Sector Antenna with Self-Selecting Switching Circuit," IEICE Trans. Commun., Vol. E84-B, No. 9, pp. 2407–2412, Sept. 2001.
[9] T. Maruyama, K. Uehara, T. Hori, and K. Kagoshima, "Rigorous analysis of transient radiation mechanism of small multi-sector monopole Yagi-Uda array antenna using FDTD method," International Journal of Numerical Modeling, Vol. 12, No. 4, pp. 341–351, 1999.
[10] M. Yamamoto, K. Ishizaki, M. Muramoto, K. Sasaki, and K. Itoh, "A planar-type five-sector antenna with printed slot array for millimeter-wave and microwave wireless LANs," IEICE 2000 Int. Symp. Antenna and propagation, Vol. 1, pp. 206–208, Aug. 2000.
[11] H. Uno, Y. Saito, G. Ohta, H. Haruki, Y. Koyanagi, and K. Egawa, "A planar sector antenna suitable for small WLAN card terminal," 14th IEEE Personal, Indoor and Mobile Radio Communications (PIMRC 2003), Vol. 3, pp. 2176–2179, Sept. 2003.
[12] D. Gray, J.W. Lu, and D.V. Thiel, "Electronically steerable Yagi-Uda microstrip patch antenna array," IEEE Trans. Antennas and Propagat., Vol. 46, No. 5, pp. 605–608, May 1998.
[13] J. Huang, "Planar microstrip Yagi array antenna," IEEE Antennas and Propagat., Soc. Symp. Dig., Vol. 2, pp. 894–897, June 1989.
[14] I. Toyoda, F. Nuno, Y. Shimizu, and M. Umehira, "Proposal of 5/25-GHz dual band OFDM-based wireless LAN for high-capacity broadband communications," The 16th Annual IEEE International Symposium on Personal, Indoor and Mobile Radio Communications (PIMRC 2005), I02-05, Vol. 3, pp. 2104–2108, Sept. 2005.

Naoki Honma
Research Engineer, Wireless Systems Innovation Laboratory, NTT Network Innovation Laboratories.
He received the B.E., M.E., and Ph.D degrees in electrical engineering from Tohoku University, Miyagi, in 1996, 1998, and 2005, respectively. In 1998, he joined NTT Radio Communication Systems Laboratories. His current research interests include planar antennas for high-speed wireless communication systems. He is a member of IEEE and the Institute of Electronics, Information and Communication Engineers (IEICE) of Japan. He received the 2003 Young Engineers Award from IEICE, the 2003 APMC Best Paper Award, and the 2006 IEICE Communications Society Best Paper Award.

Tomohiro Seki
Research Engineer, Wireless Systems Innovation Laboratory, NTT Network Innovation Laboratories.
He received the B.E., M.E., and Dr.Eng. degrees in electrical engineering from Tokyo University of Science, Tokyo, in 1991, 1993, and 2006, respectively. Since joining NTT in 1993, he has been engaged in research on planar antennas and active integrated antennas for the millimeter-wave and microwave bands. He is currently interested in system-in-package technologies for millimeter-wave communication systems. He is a member of IEEE and IEICE. He received the 1999 Young Engineer Award from IEICE and the 2006 IEICE Communications Society Best Paper Award.

Kenjiro Nishikawa
Senior Research Engineer, Wireless Systems Innovation Laboratory, NTT Network Innovation Laboratories.
He received the B.E. and M.E. degrees in welding engineering and the Dr.Eng. degree in communication engineering from Osaka University, Osaka, in 1989, 1991, and 2004, respectively. In 1991, he joined NTT Radio Communication Systems Laboratories (now NTT Network Innovation Laboratories), where he has been engaged in R&D of 3D and uniplanar MMICs on Si and GaAs and their applications. He is currently interested in millimeter-wave transceivers, system-in-package technologies, active integrated antennas, and high-speed communication systems. He is a Technical Program Committee Member of the IEEE Compound Semiconductor IC Symposium, the IEEE Radio and Wireless Symposium, and the IEEE MTT-S International Microwave Symposium. He served on the Steering Committee of the 2006 Asia-Pacific Microwave Conference. He is a member of IEEE and IEICE. He received the 1996 Young Engineer Award and the 2006 IEICE Communication Society Best Paper Award from IEICE.

Shuji Kubota
Director, Vice President, Wireless Systems Innovation Laboratory, NTT Network Innovation Laboratories.
He received the B.E. degree from the University of Electro-Communications, Tokyo, in 1980 and the Ph.D. degree in engineering from Osaka University, Osaka, in 1995. Since joining Nippon Telegraph and Telephone Public Corporation (now NTT) in 1980, he has been engaged in R&D of forward error correction schemes and modulation-demodulation schemes for satellite and personal communication systems (PHS), software-defined radio systems, wireless LAN systems, wireless access systems, and wide-area sensor network systems. During 1991–1992, he was a Visiting Researcher at the University of California, Davis. He is a member of IEEE and IEICE.